



Escherichia coli K88 activates NLRP3 inflammasome-mediated pyroptosis *in vitro* and *in vivo*

Yuanzhi Cheng^{a,b,1}, Xiao Xiao^{a,c,1}, Jie Fu^{a,b}, Xin Zong^{a,b}, Zeqing Lu^{a,b}, Yizhen Wang^{a,b,*}

^a Key Laboratory of Molecular Animal Nutrition (Zhejiang University), Ministry of Education, Hangzhou, 310058, China

^b Key Laboratory of Animal Nutrition and Feed Science (Eastern of China), Ministry of Agriculture and Rural Affairs, Hangzhou, 310058, China

^c Key Laboratory of Applied Technology on Green-Eco-Healthy Animal Husbandry of Zhejiang Province, Zhejiang A&F University, Hangzhou, 311300, China

ARTICLE INFO

Keywords:

Escherichia coli K88
Pyroptosis
LPS
C57BL/6 mouse
J774A.1 cells

ABSTRACT

Pyroptosis induced by lipopolysaccharide (LPS) has an obvious impact on intestinal inflammation and immune regulation. Enterotoxigenic *Escherichia coli* (ETEC) K88 has been proved to induce inflammatory responses in several models, but whether *E. coli* K88 participates in the same process of pyroptotic cell death as LPS remains to be identified. We conducted a pilot experiment to confirm that *E. coli* K88, instead of *Escherichia coli* O157 and *Salmonella typhimurium*, promotes the secretion of interleukin-1 beta (IL-1 β) and interleukin-18 (IL-18) in macrophages. Further experiments were carried out to dissect the molecular mechanism both *in vitro* and *in vivo*. The Enzyme-Linked Immunosorbent Assay (ELISA) results suggested that *E. coli* K88 treatment increased the expression of pro-inflammatory cytokines IL-18 and IL-1 β in both C57BL/6 mice and the supernatant of J774A.1 cells. Intestinal morphology observations revealed that *E. coli* K88 treatment mainly induced inflammation in the colon. Real-time PCR and Western blot analysis showed that the mRNA and protein expressions of pyroptosis-related factors, such as NLRP3, ASC, and Caspase1, were significantly upregulated by *E. coli* K88 treatment. The RNA-seq results confirmed that the effect was associated with the activation of NLRP3, ASC, Caspase1, GSDMD, IL-18, and IL-1 β , and might also be related to inflammatory bowel disease and the tumor necrosis factor pathway. The pyroptosis-activated effect of *E. coli* K88 was significantly blocked by NLRP3 siRNA. Our data suggested that *E. coli* K88 caused inflammation by triggering pyroptosis, which provides a theoretical basis for the prevention and treatment of ETEC in intestinal infection.

1. Introduction

Enterotoxigenic *Escherichia coli* (ETEC) remains an important cause of diarrhea in neonatal and post-weaning animals [1]. After colonizing the intestine, ETEC secretes enterotoxins and triggers an immune reaction, which results in the excessive secretion of proinflammatory cytokines, water and electrolytes, ultimately causing inflammation, barrier injury and diarrhea [2–4]. ETEC infection also leads to cell death and tissue damage [5]. The level of knowledge of these factors determines the success of therapy for ETEC infection.

Pyroptosis, as one kind of inflammatory cell deaths, can induce strong inflammatory responses to prevent pathogenic infections [6]. The biological process has been deemed as Caspase1-mediated inflammatory cell death in response to various inflammatory stimulations, including lipopolysaccharide (LPS), pathogen-associated molecular patterns, and

pH imbalance for a long time [7]. Inflammasomes are triggered and serve as platforms for the recruitment and activation of Caspase1 [8]. Typically, NLRP3 inflammasome are assembled in response to priming signals from membranous receptors, such as Toll-like receptor (TLR) and NOD-like receptor, which mediate the production of inflammatory cytokines interleukin-1 beta (IL-1 β) and interleukin-18 (IL-18) in inflammatory disorders [9,10].

Recent studies have reported that pyroptosis can be triggered by specific pathogenic bacteria, most of which are Gram-negative bacteria. Wu et al. [11] investigated that *Listeria* activated the proinflammatory Caspase1 and induced the secretion of IL-1 β and IL-18. Similar results that Caspase1-dependent IL-1 β production was induced in macrophages separately by *Clostridium difficile* and *Yersinia* were demonstrated in other studies [12,13]. Zong et al. [14] reported that *Salmonella* infection reduced GLP-1 secretion by inducing pyroptosis of intestinal L cells. In

* Corresponding author. Key Laboratory of Molecular Animal Nutrition (Zhejiang University), Ministry of Education, Hangzhou, 310058, China.

E-mail address: yzwang321@zju.edu.cn (Y. Wang).

¹ These authors contributed equally to this work.

contrast, few reports exist on Gram-positive pathogens. Research showed that *Shigella flexneri* with the virulence factor invasion plasmid antigen B induced macrophage cell death [15]. In the early stage of infection by intracellular bacterial pathogen *Brucella*, both Caspase1 and Caspase 11 were found to initiate joint inflammation and proinflammatory cytokine IL-18 production, which eventually restricted the infection [16]. Yang et al. [17] revealed that enterohemorrhagic *Escherichia coli*, *Salmonella typhimurium*, *Shigella flexneri* and *Burkholderia* spp. can induce robust inflammasome activation in both human monocyte-derived and mouse bone marrow macrophages. Studies also showed that LPS and toxin secreted by enterohemorrhagic *Escherichia coli* could activate Caspase 4, gasdermin D (GSDMD) and NLRP3 inflammasome in human THP-1 macrophages [18]. Dufies et al. [19] indicated that CNF1 toxin from uropathogenic *E. coli* targeted Rho-GTPase and then triggered the activation of Caspase1 in primary bone-marrow-derived macrophages isolated from BALB/c mice. Nevertheless, to the best of our knowledge, few studies have focused on whether ETEC activates pyroptosis.

Escherichia coli K88 is a typical kind of ETEC expressing K4 adhesin [20], which has been widely used to construct inflammation models in piglets [21], broilers [22], mice [23], epithelial cells [24], and macrophages [25]. Our previous studies identified that *E. coli* K88 treatment upregulated the expression of reactive oxygen species and inducible nitric oxide synthase in RAW264.7 cells [26], promoted the inflammatory response, and disrupted the intestinal barrier in mice [27,28]. A recent study found that the mRNA expressions of NLRP3, Caspase1, ASC and GSDMD were upregulated in porcine jejunum epithelial cells infected by *E. coli* K88 [29]. These results support that *E. coli* K88 treatment may activate pyroptosis, whereas further working are needed to explore this effect regarding the appropriate dosage, treatment time and mechanism of *E. coli* K88 both *in vivo* and *in vitro*.

Herein, we aimed to illustrate the pyroptosis-activated ability of *E. coli* K88 and the underlying mechanism by using RT-PCR, Western blot, RNA-seq, and other assays. Based on our pilot experiment, we discovered that, compared to enterohemorrhagic *Escherichia coli* O157 and *Salmonella typhimurium*, only *E. coli* K88 treatment had the same effect as LPS in enhancing the levels of IL-1 β and IL-18 in the supernatant of J774A.1 cells. Subsequently, our main findings are as follows: (i) we confirmed that treatment with 1×10^9 CFU/mL *E. coli* K88 for 12 h could improve the IL-1 β content in the serum and induce inflammation in the colon; (ii) *E. coli* K88 significantly upregulated the mRNA expression of NLRP3, Caspase1, GSDMD, ASC, IL-1 β , and IL-18, as well as the protein expression of NLRP3 and Caspase1 in the colon; (iii) our results revealed that treatment with 3×10^7 CFU/mL *E. coli* K88 for 2.5 h remarkably increased both the mRNA and protein expressions of NLRP3 in J774A.1 cells; (iv) we verified the expression of pyroptosis-related genes and identified the potentially activated pathways by RNA-seq; and (v) we confirmed that *E. coli* K88 relied on NLRP3 to trigger pyroptosis by RNA interference. We believe that these results help researchers to further reveal the specific mechanism of how the body resists ETEC infection.

2. Materials and methods

2.1. Materials

Phosphate buffer powder (PBS) was purchased from Sinopharm Chemical Reagent Co. Ltd. (Shanghai, China). Lipopolysaccharide (LPS, L2630) and adenosine triphosphate (ATP, P8232) were obtained from Sigma-Aldrich (St. Louis, MO, USA). *Escherichia coli* O157, *Escherichia coli* K88 and *Salmonella typhimurium* were maintained in our laboratory. IL-1 β (D721017) and IL-18 (D721113) ELISA kits were purchased from Sangon Biotech (Shanghai, China). Primary antibodies NLRP3, ASC, IL-1 β were acquired from Cell Signaling Technology (Danvers, USA). Primary antibody Caspase1 was bought from Santa Cruz (Dallas, USA). Primary antibody β -actin (ab8226) were purchased from Abcam (Cambridge, USA). The secondary anti-mouse IgG antibody and anti-rabbit

IgG antibody were obtained from EarthOx (San Francisco, USA). Dulbecco's modified Eagle's medium (DMEM) basic was purchased from Gibco BRL (Gaithersburg, USA). Fetal bovine serum (FBS) was acquired from Gemini (West Sacramento, USA). TRIzol reagent was purchased from Invitrogen (Carlsbad, USA). SYBR Green Master Mix was obtained from Roche (Basel, Switzerland). ECL and BCA assay kit was purchased from KeyGEN BioTECH (Nanjing, China).

2.2. Animal treatment and sample collection

Thirty C57BL/6 male mice (3 weeks of age) were obtained from the Laboratory Animal Center of Zhejiang University. All mice were housed in plastic cages on a layer of wood shavings with chow diet and water ad libitum under standard conditions. The animals were allowed to adapt to the environment for 1 week before the experiment. As shown in Fig. 1B, the mice were randomly divided into three groups of 10 each: Control group (CON, 100 μ L of LB broth for intragastric gavage, 100 μ L PBS for intraperitoneal injection), K88 group (100 μ L of 10^9 CFU/mL K88 for intragastric gavage, 100 μ L of PBS for intraperitoneal injection), and LPS group (100 μ L of LB broth for intragastric gavage, 100 μ L of 20 mg/kg body weight LPS for intraperitoneal injection).

After treatment with *E. coli* K88 or LPS for 12 h, the mice were killed by cervical dislocation. Then, serum and peritoneal lavage fluids were collected. In addition, part of the intestine was fixed in 4% paraformaldehyde, and the remaining intestinal tissues were quickly frozen and stored at -80 $^{\circ}$ C until analysis. The animal experiments were approved by the Animal Care and Use Committee of Zhejiang University and followed the institutional guidelines.

2.3. Intestinal morphology

Formalin-fixed and paraffin-embedded tissues were cut into 4 μ m thick sections, followed by slicing and staining with hematoxylin and eosin (H & E). Images of the slices were obtained using the Leica DM3000 Microsystem (Wetzlar, Germany).

2.4. Cell culture

The mouse macrophage cell line J774A.1, a generous gift from Prof. Houhui, Song (College of Animal Science and Technology, Zhejiang A & F University), was cultured in complete Gibco DMEM basic medium (containing 10% FBS, 100 μ g/mL penicillin and 100 μ g/mL streptomycin) at 37 $^{\circ}$ C in a humidified incubator with 5% CO₂.

2.5. Cell experiment design

A total of 10^6 cells were seeded into six-well plates and allowed to adhere for 18–24 h before treatment.

As shown in Fig. 1A, for the pilot experiment, samples of the *Escherichia coli* O157 (O157) group, *Escherichia coli* K88 (K88) group and *Salmonella typhimurium* (STM) group were incubated with 1 mL DMEM basic culture containing 3×10^7 CFU/mL corresponding pathogenic strain, whereas the LPS group was treated with 1 mL DMEM basic culture containing 0.5 μ g/mL LPS. After incubation for 2 h, cultures in the O157 group, K88 group and STM group were added with 2 mmol/L ATP for 30 min. As for the LPS group, ATP was added 4 h after LPS treatment for 30 min.

2.6. Enzyme-linked immunosorbent assay (ELISA) for cytokines

The serum and the peritoneal lavage fluid from mice and the supernatant from J774A.1 cell culture were collected. The levels of IL-1 β and IL-18 were determined according to the manufacturer's instructions.

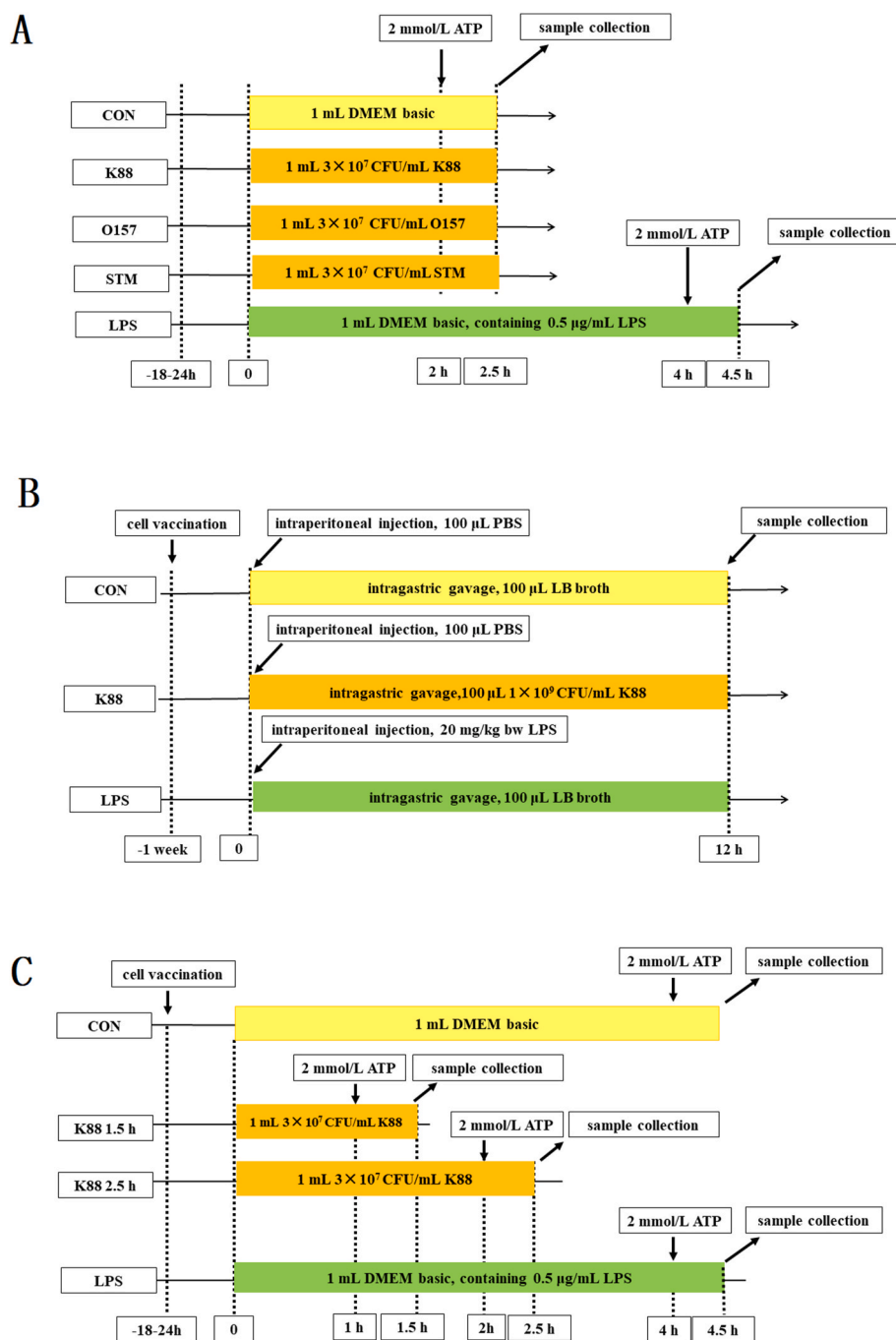


Fig. 1. Designs of (A) pilot experiment, (B) *in Vivo* experiment, and (C) *in Vitro* experiment.

2.7. Real-time PCR

Total RNA was extracted by TRIzol reagent and determined by NanoDrop 2000 (Thermo Scientific, USA). cDNA was generated by reverse transcription using 2 μ g of RNA. Real-time PCR was performed using the StepOne Plus™ system (Applied Biosystems, USA). The primers of *nlrp3*, *asc*, *caspase1*, *gsdmd*, *il-1 β* , *il-18*, and *18s* were listed in Table 1. The relative gene expression was calculated using the $2^{-\Delta\Delta Ct}$ method and presented after comparison with the endogenous control gene *18 S*.

2.8. Western blot analysis

The total proteins of colon and cell were extracted and quantified

using the BCA kit according to the manufacturer's instructions. Proteins with different molecular weight were separated via 10% SDS-PAGE and blotted onto nitrocellulose membranes. After incubation in 5% skimmed milk powder at RT for 1 h, the membranes were incubated with the primary antibodies overnight at 4 °C, followed by incubation in HRP-conjugated anti-rabbit or anti-mouse IgG for 1 h. The results were quantified by Image J software.

2.9. RNA-seq

A total amount of 1 μ g RNA from the J774A.1 cell line was collected and prepared into a cDNA library. The transcriptome assembly and annotation protocols were provided by Novogene Biotechnology (Beijing, China). The generated cDNA library was sequenced to paired-end

Table 1
Primer sequences for real-time PCR.

Gene	Sequence (5'→ 3')	GenBank No.
Nlrp3	Forward: GACACGAGTCTGGTACTT Reverse: TTCTCGGGGGTAATCTTC	NM_145827.4
Asc	Forward: CTGCAGATGGACGCCATAGA Reverse: GTGAGCTCCAAGCCATACGA	NM_023258.4
Caspase1	Forward: GGACTGACTGGGACCCTCAA Reverse: GAGGGCAAGACGTGTACGAG	NM_009807.2
Gsdmd	Forward: TGGTGAAGCACGCTTTGGAA Reverse: GTGGGGATCAGAGACGTTGG	NM_026960.4
IL-1 β	Forward: TGCCACCTTTTGACAGTGATG Reverse: ATGTGCTGCTGCGAGATTG	NM_008361.4
IL-18	Forward: ACAAGTTTACAAGCATCCAGGCAC Reverse: GGAAGGTTTGAGGCGGCTTT	NM_008360.2
18 S	Forward: CGAGGGTTTCGGGATTTGTG Reverse: AAAGCCAACCCGAGCGTC	NR_046233.2

150 bp read length using HiSeq 2500 (Illumina, USA) according to the manufacturer's instructions to a depth of 40–50 million reads. Differential expression analysis of CON, K88, and LPS groups was performed using the R package DESeq2 (Bioconductor, USA). Genes with an adjusted $P < 0.05$ were assigned as differentially expressed.

The raw reads were pre-processed with FASTQC (Babraham Bioinformatics, UK) followed by sequence alignment using HISAT2 according to the method of Kim et al. [30]. The transcript levels were converted to the log-space by taking the logarithm to base 2. R studio was used to run custom R scripts to perform box plots, scatter plots, dendrograms, and heatmaps. Gene Ontology (GO) enrichment analysis of differentially expressed genes (DEGs) was applied using the clusterProfiler R package. The GO terms of differential expressed genes with corrected $P < 0.05$ were significantly enriched and assessed in the Kyoto Encyclopedia of Genes and Genomes (KEGG) pathways.

2.10. Transfection of siRNA

The NLRP3 siRNA (No. siG 1161091244-1-5) and scramble siRNA used in this study were chemically synthesized by Ribo Biotechnology (Ribobio, China). siRNA was transfected into IPEC-J2 cells using the Lipofectamine 3000 kit (Thermo Scientific, USA) according to the manufacturer's protocol.

2.11. Statistical analysis

All data were expressed as means \pm standard deviation (SD) and processed by GraphPad Prism 8.0 (GraphPad Software, Inc., San Diego, CA, USA). Quantitative analysis of the fluorescence intensity was performed using ImageJ. One-way analysis of variance (ANOVA) followed by least significant difference multiple comparison test was used, and $P < 0.05$ was considered as statistically significant.

3. Results

3.1. Pilot experiment: *E. coli* K88 treatment improved the levels of IL-1 β and IL-18 in the supernatant of J774A.1 cells

In order to validate the pyroptosis-activating effect of pathogenic bacteria, a pilot experiment was conducted to measure the pro-inflammatory cytokine levels in the supernatant of J774A.1 cells using ELISA. As shown in Fig. 2, compared to the CON group, cells exposed to *E. coli* K88 for 2.5 h and LPS for 4.5 h showed a significant increase in the IL-1 β and IL-18 levels ($P < 0.0001$). Pretreatment with STM had the same effect ($P < 0.01$), while O157 did not affect the cytokine levels. Thus, *E. coli* K88 and LPS were used in subsequent experiments.

3.2. *E. coli* K88 treatment improved the levels of IL-1 β and IL-18 in the serum and peritoneal lavage fluid of C57BL/6 mice

As shown in Fig. 3A and B, compared with the CON group, the IL-1 β content was remarkably increased in the serum of C57BL/6 mice after treatment with K88 and LPS ($P < 0.0001$), whereas only LPS promoted the IL-1 β content in the peritoneal lavage fluid ($P < 0.01$). LPS treatment increased the serum IL-18 content from $5.17 \pm 0.62 \mu\text{g/mL}$ (CON group) to $7.13 \pm 0.43 \mu\text{g/mL}$ ($P < 0.01$), while both *E. coli* K88 and LPS treatments significantly increased the IL-18 content in the peritoneal lavage fluid ($P < 0.01$).

3.3. *E. coli* K88 treatment induced inflammation in the colon of C57BL/6 mice

As shown in Fig. 4, the intestinal morphology analysis of the CON group showed orderly arranged intestinal epithelial cells and intact mucus layers. LPS treatment resulted in atrophied villus in the duodenum, jejunum and colon, with discontinuous brush borders and disarrayed epithelium, which was the result of intestinal epithelial cell death. *E. coli* K88 treatment only caused colon injury. Nevertheless, the mucus layers of the ileum were intact and smooth, indicating that LPS and *E. coli* might not induce intestinal epithelial cell shedding in the ileum (Fig. 4C).

3.4. *E. coli* K88 treatment upregulated pyroptosis-related gene and protein expressions in the colon of C57BL/6 mice

The results in Fig. 5A–F illustrated that the mRNA levels of pyroptosis-related genes were significantly increased in the colon after *E. coli* K88 and LPS treatment. Specifically, LPS treatment upregulated the expressions of NLRP3, Caspase1, ASC, GSDMD, IL-1 β , and IL-18 b y 148-fold ($P < 0.01$), 6.0-fold ($P < 0.0001$), 5.1-fold ($P < 0.001$), 3.1-fold ($P < 0.0001$), 4.1-fold ($P < 0.0001$), and 2.9-fold ($P < 0.0001$). Furthermore, *E. coli* K88 treatment upregulated the expressions of NLRP3, Caspase1, ASC, GSDMD, IL-1 β , and IL-18 b y 17.7-fold ($P < 0.01$), 2.6-fold ($P < 0.05$), 4.1-fold ($P < 0.01$), 2.7-fold ($P < 0.001$), 3.1-fold ($P < 0.001$), and 2.1-fold ($P < 0.01$). Meanwhile, compared to the

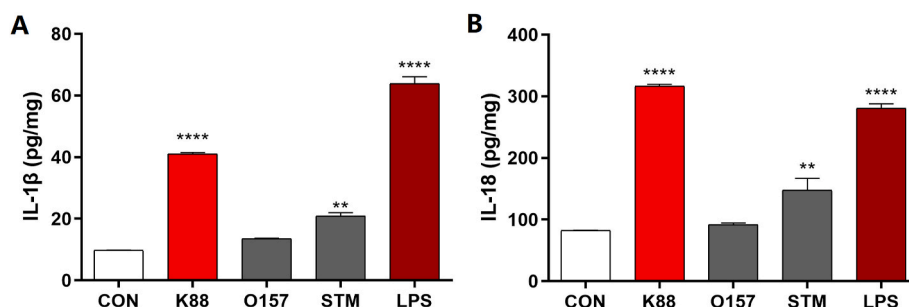


Fig. 2. Pro-inflammatory cytokine levels in the supernatant of J774A.1 b y ELISA (n = 6). (A) IL-1 β , and (B) IL-18.

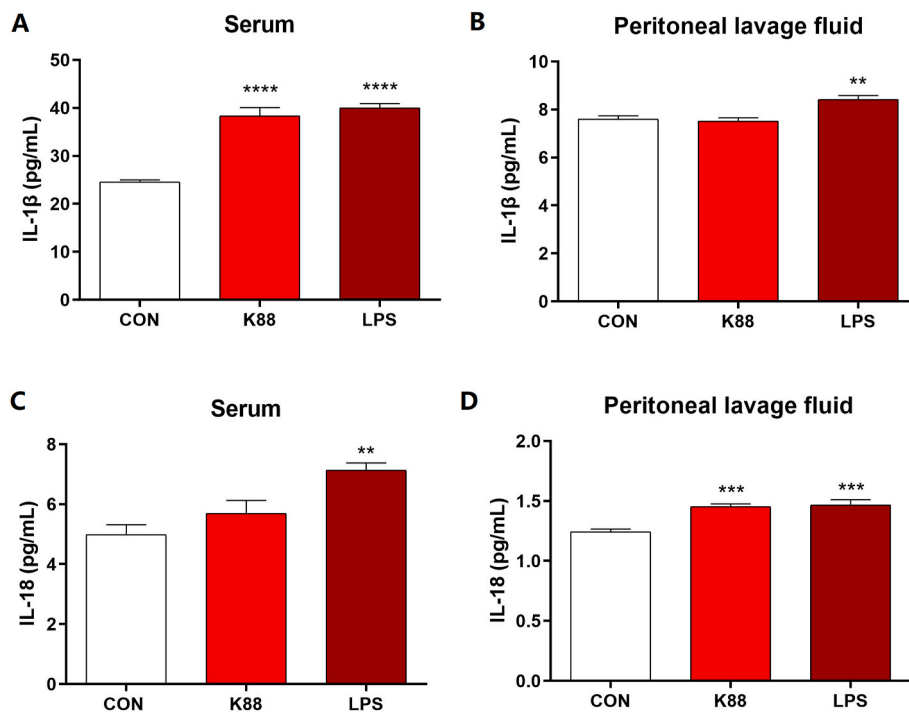


Fig. 3. Pro-inflammatory cytokine levels in the serum and peritoneal lavage fluid of C57BL/6 mice by ELISA (n = 6). (A) IL-1 β levels in the serum, (B) IL-1 β levels in the peritoneal lavage fluid, (C) IL-18 levels in the serum, and (D) IL-18 levels in the peritoneal lavage fluid (*P < 0.05, **P < 0.01, ***P < 0.001, ****P < 0.0001).

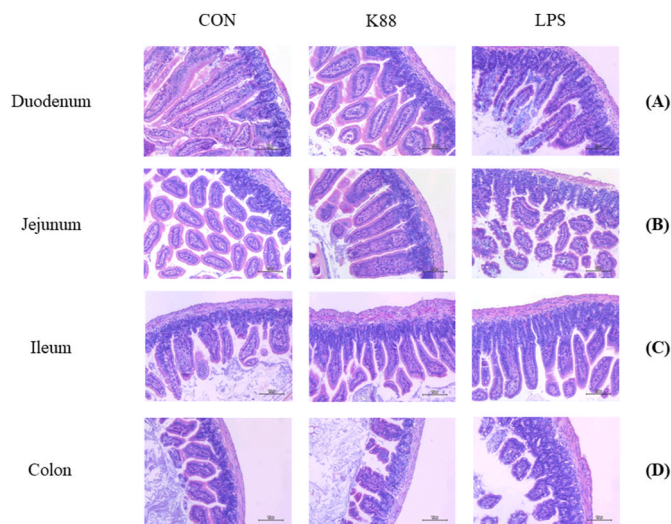


Fig. 4. Effects of K88 and LPS on the intestinal morphology in the (A) duodenum, (B) jejunum, (C) ileum, and (D) colon by H&E at 200 \times magnification.

CON group, *E. coli* K88 treatment enhanced the protein expression of NLRP3, Caspase1, and ASC, exhibiting a similar tendency as LPS (Fig. 5G).

3.5. *E. coli* K88 treatment upregulated pyroptosis-related gene and protein expressions in J774A.1

As shown in Fig. 6A–D, the activity of NLRP3 was significantly elevated in response to *E. coli* K88 and LPS, with the 2.5 h *E. coli* K88 treatment being the most efficient. In addition, *E. coli* K88 and LPS markedly elevated the activity of IL-1 β , whereas neither of them made an influence on the expression of Caspase1 and GSDMD.

The Western blot results revealed that LPS and 2.5 h *E. coli* K88

treatment significantly increased the expression of Caspase1 and IL-1 β in the supernatant of J774A.1 cells, but not in the cell lysate (Fig. 6E). Meanwhile, LPS and 2.5 h *E. coli* K88 treatment significantly enhanced the expression of NLRP3 and ASC in the cell lysate. Treatment with 1.5 h *E. coli* K88 did not promote the expression of pyroptosis-related protein. Subsequently, treatment with 3×10^7 CFU/mL *E. coli* K88 for 2.5 h was selected for the RNA-seq experiment.

3.6. RNA-seq

In order to explore how the pyroptosis-related genes were altered upon *E. coli* K88 and LPS treatment, we applied RNA-seq to map the transcriptional changes and potential pathways. The heatmap results (Fig. 7A) showed that *E. coli* K88 and LPS treatment significantly increased the expression of pyroptosis-related genes, which were mostly consistent with our RT-PCR results (Fig. 6A–D). We found 7085 differentially expressed genes, of which 3565 were upregulated, including IL-18 and IL-1 β (shown in yellow), whereas 3520 were downregulated upon *E. coli* K88 and LPS treatment (Fig. 7B). Importantly, the pathways in which upregulated genes were enriched correlated with inflammation-related pathways including TNF signaling, NF-kappa B signaling, cytokine-cytokine receptor interaction, and JAK-STAT signaling pathways based on the KEGG analysis (Fig. 7D).

3.7. NLRP3 siRNA abolished the apoptosis-activated effects of *E. coli* K88

A specific siRNA was used to knock down NLRP3 expression. As shown in Fig. 8A, NLRP3 siRNA-treated groups exhibited lower levels of NLRP3 mRNA expression than the negative control. When the cells were challenged with *E. coli* K88, the apoptosis-activated effect was significantly blocked by NLRP3 siRNA (Fig. 8B and C).

4. Discussion

The gastrointestinal tract is a complex ecosystem composed of epithelial cells, immune cells, intestinal stem cells, and microbiota [31].

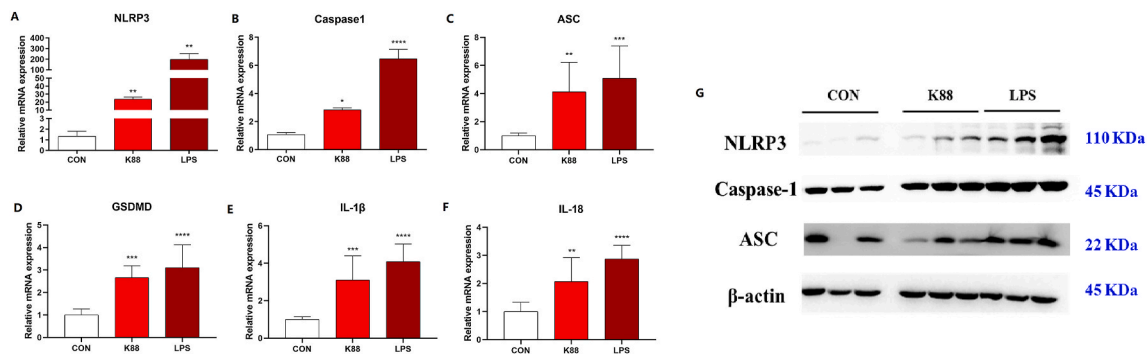


Fig. 5. Pyroptosis-related gene and protein expressions in the colon of C57BL/6 mice. (A) relative mRNA expression of NLRP3 (n = 6), (B) relative mRNA expression of Caspase1 (n = 8), (C) relative mRNA expression of ASC (n = 8), (D) relative mRNA expression of GSDMD (n = 8), (E) relative mRNA expression of IL-1β (n = 8), (F) relative mRNA expression of IL-18 (n = 8), and (G) Western blot analysis of NLRP3, Caspase1 and ASC (n = 3) (*P < 0.05, **P < 0.01, ***P < 0.001, ****P < 0.0001).

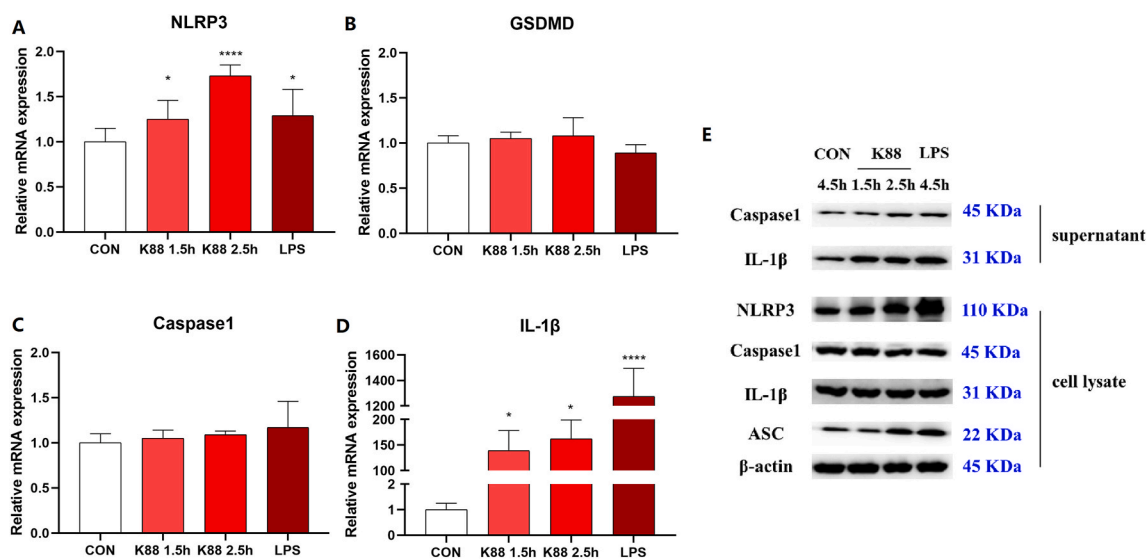


Fig. 6. Pyroptosis-related gene and protein expressions in J774A.1 cells. (A) relative mRNA expression of NLRP3 (n = 9), (B) relative mRNA expression of GSDMD (n = 9), (C) relative mRNA expression of Caspase1 (n = 9), (D) relative mRNA expression of IL-1β, (E) relative mRNA expression of IL-18 (n = 9), and (F) Western blot analysis of NLRP3, Caspase1, IL-1β and ASC in the supernatant and cell lysate (*P < 0.05, **P < 0.01, ***P < 0.001, ****P < 0.0001).

During extended exposure to various antigens including pathogens and toxins, the sensitive and fragile intestinal homeostasis can be disturbed [32]. Specifically, the host can activate immune response, intestinal inflammation, and cell death against inflammatory stimuli [33]. Pyroptosis is one of programmed cell death modes necessary for the innate immune system to fight against intracellular pathogens by preventing pathogen replication and exposing pathogens to extracellular killing mechanisms [34]. Numerous studies have demonstrated that NLRP3, triggered by LPS and certain enteric pathogens, assembles Caspase1 through adapter protein ASC, which in turn promotes the activation of inflammasomes and secretion of mature proinflammatory cytokines IL-18 and IL-1β [35–38]. A recent study revealed that piglets challenged with ETEC activated the release of Caspase1 and the cleavage of porcine GSDMD in the duodenum and jejunum [39], supporting that ETEC was able to trigger pyroptosis *in Vivo*. Loss et al. [40] found that, compared to 20 ng/mL of LPS treatment alone, 20 ng/mL of LPS plus 10^7 CFU/mL ETEC treatment enhanced the mRNA expression of IL-1β and NLRP3, while it had no effect on that of ASC, IL-18 and Caspase1 in porcine monocyte-derived dendritic cells. Since no separate ETEC group was set in the study from Loss et al. it could not be determined whether ETEC was the decisive factor or it only enhanced the pyroptosis-activating ability of LPS. Therefore, it is worthwhile to

further examine the correlation between ETEC, intestinal inflammation, and the activation of NLRP3 inflammasome by different models.

As shown in Fig. 2, our pilot experiment revealed that *E. coli* K88 possessed better ability to promote cytokine secretion than *Escherichia coli* O157 and *Salmonella typhimurium* in J774A.1 macrophages, which is one of the most widely used models to mimic pathological pyroptotic cells *in Vitro* [41]. *E. coli* O157, a notorious enterohemorrhagic *Escherichia coli*, is among the most common serotypes that can cause acute gastroenteritis, hemorrhagic colitis, and hemolytic-uremic syndrome [42]. To date, few studies have pointed out that *E. coli* O157 can trigger pyroptosis. Only Xue et al. reported that *E. coli* O157 could be used to create an NLRP3-activated model in Caco-2 cells, in which they revealed the pyroptosis suppressing functions of quercetin [43] and raspberry extract [44]. In this study, we did not find a similar effect of *E. coli* O157 on J774A.1 cells. Moreover, although *Salmonella typhimurium*, whose pyroptosis-activated ability had been reported in several studies [45–47], increased the levels of IL-1β and IL-18, which were still lower than those of *E. coli* K88 infection under same treatment conditions.

Therefore, an *in Vivo* model of C57BL/6 mice was set up to investigate the pyroptosis-activating ability of *E. coli* K88. The cytokine contents in peritoneal lavage fluid and serum can reflect the inflammation-inducing effect. As shown in Fig. 3, LPS strongly stimulated the

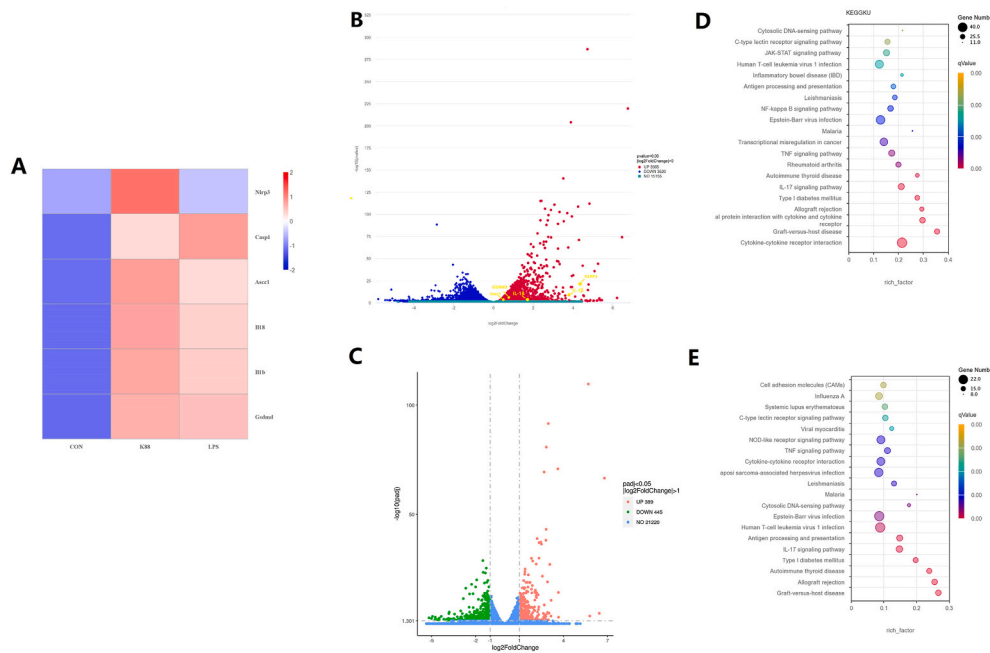


Fig. 7. RNA-seq analysis of differentially expressed genes in the CON, K88 and LPS group. (A) Heatmap of pyroptosis-related genes expression levels; (B) volcano map of differentially expressed genes between the K88 and CON groups; (C) volcano map of differentially expressed genes between the LPS and CON groups; (D) KEGG map of relative pathways between the K88 and CON groups; and (E) KEGG map of relative pathway between the LPS and CON groups.

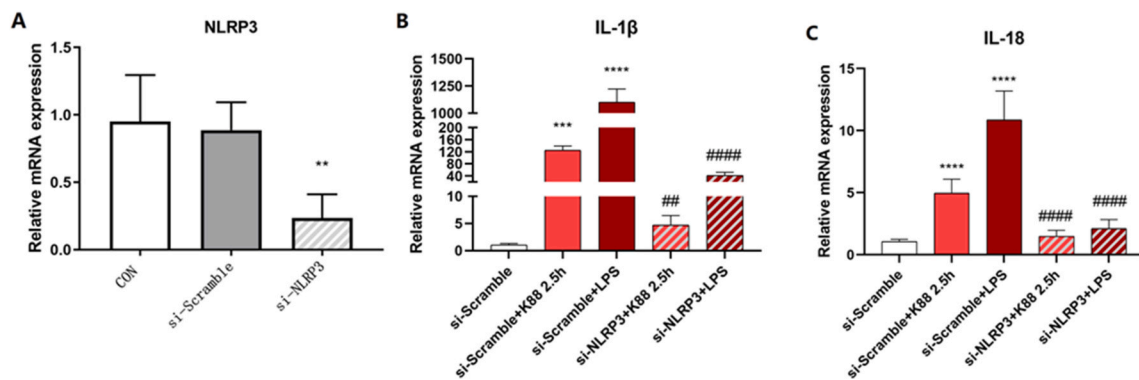


Fig. 8. NLRP3 knockdown abolished the apoptosis-activated effects of *E. coli* K88. (A) qPCR result of NLRP3 mRNA expression level, (B) relative mRNA expression of IL-1 β (n = 8), and (C) relative mRNA expression of IL-18. (*P < 0.05, **P < 0.01, ***P < 0.001, ****P < 0.0001, compared with scramble siRNA-treated cells; #P < 0.05, ##P < 0.01, ###P < 0.001, ####P < 0.0001, compared with NLRP3 siRNA-treated cells).

productions of IL-1 β and IL-18 both in the serum and peritoneal lavage fluid. However, *E. coli* K88 induced a considerably weaker but significant increase in serum IL-1 β production and IL-18 production in peritoneal lavage fluid. These results suggested that LPS induced systemic infection in the experimental animals, while *E. coli* K88 caused organ-specific infection [48]. The intestinal morphology results showed that *E. coli* K88 infection led to severe intestinal barrier injury in the colon (Fig. 4D), which was consistent with previous reports [49,50], while LPS treatment caused atrophied villus in the duodenum, jejunum, and colon. These findings indicated that a single dose of intragastric gavage with 100 μ L of 10⁹ CFU/mL K88 for 12 h specifically cause colitis injury. The expression of NLRP3 inflammasomes in the mouse colon was examined using RT-PCR and Western blot (Fig. 5), and the results confirmed that both *E. coli* K88 and LPS treatment significantly upregulated the expression of pyroptosis-related genes and proteins in the colon.

Since the complete understanding of pyroptosis-activated function requires *in Vitro* experiments, we examined the mRNA and protein expression levels of NLRP3 inflammasomes in J774A.1 macrophages exposed to *E. coli* K88. To optimize the treatment condition, two

different infection durations were chosen, and a treatment time of 2.5 h of *E. coli* K88 was selected for RNA-seq. As shown in Fig. 6C, neither *E. coli* K88 or LPS treatment influenced the expression of Caspase1 and GSDMD. However, the heatmap results indicated that *E. coli* K88 and LPS enhanced the expression of Caspase1 and GSDMD (Fig. 7A). These differences may be due to the cell state or the mRNA extraction method. Experiments such as immunofluorescence analysis and laser scanning confocal microscopy need to be performed for further clarification.

Taken together, RT-PCR and RNA-seq analysis suggested that *E. coli* K88 treatment upregulated the genes involved in the inflammation-related signaling pathways (Fig. 7D), which resulted in the secretions of IL-1 β and IL-18 and the activation of NLRP3 inflammasome-mediated pyroptosis in macrophages (Fig. 7B). *E. coli* K88 treatment mostly triggered cytokine-cytokine receptor interaction and the TLR signaling pathway, which were crucial for macrophage activation [51]. *E. coli* K88 treatment might also trigger NF-kappa B and JAK-STAT signaling pathways, which was consistent with a previous study [52]. In addition, after NLRP3 gene was interfered by siRNA, the effect of *E. coli* K88 treatment on activating pyroptosis was inhibited, since the expressions

of IL-1 β and IL-18 were significantly downregulated (Fig. 8B and C). However, the precise mechanism underlying the metabolic effects of *E. coli* K88 on macrophages requires further research.

Further experimentation is needed to explore the mechanism of *E. coli* K88 activated NLRP3 inflammasomes. One possibility is that the strain itself is recognized by membrane protein receptors. Zong et al. [14] discovered that *Salmonella* induced the pyroptosis of enteroendocrine L cells by activating the TLR4/NF-kappa B/NLRP3 pathway. Harvest and Miao [53] revealed that *Burkholderia thailandensis* can invade the cytosol and trigger the pyroptosis of infected cells. Another possibility is that the bacterial effector proteins can trigger pyroptosis. Rathinam et al. [54] demonstrated that the combination of LPS plus cholera toxin B can trigger the NLRP3 inflammasome-mediated release of IL-1 β by bone marrow macrophages derived from C57BL/6 mice but not by those derived from the 129 strain of mice. Liu et al. [36] indicated that *Giardia duodenalis* and its secreted protein peptidyl-prolyl *cis*-trans isomerase B were able to induce macrophage pyroptosis and promote the release of the proinflammatory cytokines IL-1 and IL-18 through the TLR4 pathway. Deo et al. [55] revealed that macrophages exposed to toxins and outer membrane vesicles from *Neisseria gonorrhoeae*, uropathogenic *Escherichia coli* and *Pseudomonas aeruginosa* induce mitochondrial apoptosis and NLRP3 inflammasome activation. Interestingly, several pathogenic bacteria are able to express specific genes to attenuate pyroptosis, so that they can evade the immune system. In addition, Zuo et al. [56] revealed that *Salmonella* plasmid virulence C gene in *Salmonella typhimurium* inhibits pyroptosis and intestinal inflammation to promote bacterial dissemination. Santos et al. [57] reported that interferon-induced guanylate-binding proteins are required for non-canonical inflammasome activation by cytosolic *Salmonella* or upon cytosolic delivery of LPS. *E. coli* K88 was able to adhere the epithelial cells due to its fimbrial adhesion K88 [58], and activate the NF-kappa B/P38 signaling pathway [52], TLRs signaling pathway [59], and JNK pathway [25], etc. In follow-up research, we aim to investigate the key role of *E. coli* K88 in dependent cell death.

Funding

This research was funded by The National Natural Science Foundation of China (U21A20249), China Postdoctoral Science Foundation (2023M733150) and China Agriculture Research System of MOF and MARA (CARS-35).

Availability of data and materials

The datasets generated and analyzed during the current study are not publicly available. Please contact the authors for data requests.

Consent for publication

Not applicable.

Ethics approval and consent to participate

Not applicable.

CRedit authorship contribution statement

Yuanzhi Cheng: Data curation, Investigation, Writing – original draft. **Xiao Xiao:** Investigation, Software, Funding acquisition. **Jie Fu:** Visualization. **Xin Zong:** Conceptualization, Supervision. **Zeqing Lu:** Conceptualization. **Yizhen Wang:** Funding acquisition, Supervision, Writing – review & editing.

Declaration of competing interest

The authors declare that they have no known competing financial

interests or personal relationships that could have appeared to influence the work reported in this paper.

Data availability

Data will be made available on request.

References

- [1] V. Melkebeek, B.M. Goddeeris, E. Cox, ETEC vaccination in pigs, *Vet. Immunol. Immunopathol.* 152 (1–2) (2013) 37–42, <https://doi.org/10.1016/j.vetimm.2012.09.024>.
- [2] Y. Gong, X. Jin, B. Yuan, Y. Lv, G. Yan, M. Liu, C. Xie, J. Liu, Y. Tang, H. Gao, Y. Zhu, Y. Huang, W. Wang, G protein-coupled receptor 109A maintains the intestinal integrity and protects against ETEC mucosal infection by promoting IgA secretion, *Front. Immunol.* 11 (2020) 583652, <https://doi.org/10.3389/fimmu.2020.583652>.
- [3] A.J. Leon, J.A. Garrote, E. Arranz, Cytokines in the pathogenesis of inflammatory bowel diseases, *Med Clin-Barcelona* 127 (4) (2006) 145–152, <https://doi.org/10.1157/13090382>.
- [4] B. Nagy, P.Z. Fekete, Enterotoxigenic *Escherichia coli* (ETEC) in farm animals, *Vet. Res.* 30 (2–3) (1999) 259–284.
- [5] B. Nagy, P.Z. Fekete, Enterotoxigenic *Escherichia coli* in veterinary medicine, *Int J Med Microbiol* 295 (6–7) (2005) 443–454, <https://doi.org/10.1016/j.ijmm.2005.07.003>.
- [6] B.E. Burdette, A.N. Esparza, H. Zhu, S. Wang, Gasdermin D in pyroptosis, *Acta Pharm. Sin. B* 11 (9) (2021) 2768–2782, <https://doi.org/10.1016/j.apsb.2021.02.006>.
- [7] L.R. Zhao, R.L. Xing, P.M. Wang, N.S. Zhang, S.J. Yin, X.C. Li, L. Zhang, NLRP1 and NLRP3 inflammasomes mediate LPS/ATP-induced pyroptosis in knee osteoarthritis, *Mol. Med. Rep.* 17 (4) (2018) 5463–5469.
- [8] J. Chavarría-Smith, R.E. Vance, The NLRP1 inflammasomes, *Immunol. Rev.* 265 (1) (2015) 22–34.
- [9] S. Toldo, A.G. Mauro, Z. Cutter, A. Abbate, Inflammasome, pyroptosis, and cytokines in myocardial ischemia-reperfusion injury, *Am. J. Physiol. Heart Circ. Physiol.* 315 (6) (2018) H1553–H1568, <https://doi.org/10.1152/ajpheart.00158.2018>.
- [10] S. Toldo, E. Mezzaroma, A.G. Mauro, F. Salloum, B.W. Van Tassel, A. Abbate, The inflammasome in myocardial injury and cardiac remodeling, *Antioxidants Redox Signal.* 22 (13) (2015) 1146–1161, <https://doi.org/10.1089/ars.2014.5989>.
- [11] J.H. Wu, T. Fernandes-Alnemri, E.S. Alnemri, Involvement of the AIM2, NLRCA4, and NLRP3 inflammasomes in caspase-1 activation by *Listeria monocytogenes*, *J. Clin. Immunol.* 30 (5) (2010) 693–702.
- [12] Y.H. Liu, Y.C. Chang, L.K. Chen, P.A. Su, W.C. Ko, Y.S. Tsai, Y.H. Chen, H.C. Lai, C. Y. Wu, Y.P. Hung, P.J. Tsai, The ATP-P2X(7) signaling Axis is an essential sentinel for intracellular *Clostridium difficile* pathogen-induced inflammasome activation, *Front. Cell. Infect. Microbiol.* 8 (2018).
- [13] J. Sarhan, B.C. Liu, H.I. Muendlein, P. Li, R. Nilson, A.Y. Tang, A. Rongvaux, S. C. Bunnell, F. Shao, D.R. Green, A. Poltorak, Caspase-8 induces cleavage of gasdermin D to elicit pyroptosis during *Yersinia* infection, *P Natl Acad Sci USA* 115 (46) (2018) E10888–E10897.
- [14] Y.B. Zong, W.J. Chen, Y.S. Zhao, X.Y. Suo, X.J. Yang, *Salmonella* infection causes hyperglycemia for decreased GLP-1 content by enteroendocrine L cells pyroptosis in pigs, *Int. J. Mol. Sci.* 23 (3) (2022).
- [15] L. Senerovic, S.P. Tsunoda, C. Goosmann, V. Brinkmann, A. Zychlinsky, F. Meissner, M. Kolbe, Spontaneous formation of IpaB ion channels in host cell membranes reveals how *Shigella* induces pyroptosis in macrophages, *Cell Death Dis.* 3 (2012).
- [16] C.A. Lacey, W.J. Mitchell, A.S. Dadelahi, J.A. Skyberg, Caspase-1 and caspase-11 mediate pyroptosis, inflammation, and control of *Brucella* joint infection, *Infect. Immun.* 86 (9) (2018).
- [17] J.L. Yang, Y. Zhao, J.J. Shi, F. Shao, Human NAIP and mouse NAIP1 recognize bacterial type III secretion needle protein for inflammasome activation, *P Natl Acad Sci USA* 110 (35) (2013) 14408–14413, <https://doi.org/10.1073/pnas.1306376110>.
- [18] J.M. Platnich, H. Chung, A. Lau, C.F. Sandall, A. Bondzi-Simpson, H.M. Chen, T. Komada, A.C. Trotman-Grant, J.R. Brandelli, J. Chun, P.L. Beck, D.J. Philpott, S. E. Girardin, M. Ho, R.P. Johnson, J.A. MacDonald, G.D. Armstrong, D.A. Muruve, Shiga toxin/lipopolysaccharide activates caspase-4 and gasdermin D to trigger mitochondrial reactive oxygen species upstream of the NLRP3 inflammasome, *Cell Rep.* 25 (6) (2018), <https://doi.org/10.1016/j.celrep.2018.09.071>, 1525–U20.
- [19] O. Dufies, A. Doye, J. Courjon, C. Torre, G. Michel, C. Loubatier, A. Jacquiel, P. Chaintreuil, A. Majoor, R.R. Guinamard, A. Gallerand, P.H.V. Saavedra, E. Verhoeyen, A. Rey, S. Marchetti, R. Ruimy, D. Czerucka, M. Lamkanfi, B.F. Py, P. Munro, O. Visvikis, L. Boyer, *Escherichia coli* Rho GTPase-activating toxin CNF1 mediates NLRP3 inflammasome activation via p21-activated kinases-1/2 during bacteraemia in mice, *Nat Microbiol* 6 (3) (2021) 401.
- [20] J. Osek, Clonal analysis of *Escherichia coli* strains isolated from pigs with post-weaning diarrhea by pulsed-field gel electrophoresis, *FEMS Microbiol. Lett.* 186 (2) (2000) 327–331, [https://doi.org/10.1016/S0378-1097\(00\)00141-5](https://doi.org/10.1016/S0378-1097(00)00141-5).
- [21] R.G. Hermes, F. Molist, J.F. Perez, A.G. de Segura, M. Ywazaki, R. Davin, M. Nofrarias, T.K. Korhonen, R. Virkola, S.M. Martin-Orue, Casein glycomacropeptide in the diet may reduce *Escherichia coli* attachment to the

- intestinal mucosa and increase the intestinal lactobacilli of early weaned piglets after an enterotoxigenic *E. coli* K88 challenge, *Br. J. Nutr.* 109 (6) (2013) 1001–1012.
- [22] N.K. Emami, A. Daneshmand, S.Z. Naeini, E.N. Graystone, L.J. Broom, Effects of commercial organic acid blends on male broilers challenged with *E. coli* K88: performance, microbiology, intestinal morphology, and immune response, *Poultry Sci.* 96 (9) (2017) 3254–3263.
- [23] Q. Jiang, H.W. Zhang, Y.G. Xie, Y.Z. Wang, Recombinant expression of porcine lactoferrin peptide LF-6 with intein technology and its immunomodulatory function in ETEC K88-infected mice, *Int. Immunopharm.* 39 (2016) 181–191.
- [24] G. Gonzalez-Ortiz, S. Bronsoms, H.C.Q. Van Ufford, S.B.A. Halkes, R. Virkola, R.M. J. Liskamp, C.J. Beukelman, R.J. Pieters, J.F. Perez, S.M. Martin-Orue, A proteinaceous fraction of wheat bran may interfere in the attachment of enterotoxigenic *E. coli* K88 (F4+) to porcine epithelial cells, *PLoS One* 9 (8) (2014).
- [25] Y. Mao, B. Wang, X. Xu, W. Du, W. Li, Y. Wang, Glycyrrhizic acid promotes M1 macrophage polarization in murine bone marrow-derived macrophages associated with the activation of JNK and NF- κ B, *Mediat. Inflamm.* 2015 (2015) 372931, <https://doi.org/10.1155/2015/372931>.
- [26] S. Chen, Z.Q. Lu, F.Q. Wang, Y.Z. Wang, Cathelicidin-WA polarizes *E. coli* K88-induced M1 macrophage to M2-like macrophage in RAW264.7 cells, *Int. Immunopharm.* 54 (2018) 52–59.
- [27] Q. Jiang, H. Zhang, Y. Xie, Y. Wang, Recombinant expression of porcine lactoferrin peptide LF-6 with intein technology and its immunomodulatory function in ETEC K88-infected mice, *Int. Immunopharm.* 39 (2016) 181–191, <https://doi.org/10.1016/j.intimp.2016.07.029>.
- [28] T. Wang, J. Fu, X. Xiao, Z. Lu, F. Wang, M. Jin, Y. Wang, X. Zong, CBP22, a novel bacteriocin isolated from *Clostridium butyricum* ZJU-F1, protects against LPS-induced intestinal injury through maintaining the tight junction complex, *Mediat. Inflamm.* 2021 (2021) 8032125, <https://doi.org/10.1155/2021/8032125>.
- [29] K. Xiao, Y. Yang, Y. Zhang, Q.Q. Lv, F.F. Huang, D. Wang, J.C. Zhao, Y.L. Liu, Long-chain PUFA ameliorate enterotoxigenic *Escherichia coli*-induced intestinal inflammation and cell injury by modulating pyroptosis and necroptosis signaling pathways in porcine intestinal epithelial cells, *Br. J. Nutr.* 128 (5) (2022) 835–850, <https://doi.org/10.1017/S0007114521005092>.
- [30] D. Kim, J.M. Paggi, C. Park, C. Bennett, S.L. Salzberg, Graph-based genome alignment and genotyping with HISAT2 and HISAT-genotype, *Nat. Biotechnol.* 37 (8) (2019) 907–915, <https://doi.org/10.1038/s41587-019-0201-4>.
- [31] Q. Cao, R.T. Mertens, K.N. Sivanathan, X. Cai, P. Xiao, Macrophage orchestration of epithelial and stromal cell homeostasis in the intestine, *J. Leukoc. Biol.* 112 (2) (2022) 313–331, <https://doi.org/10.1002/JLB.3RU0322-176R>.
- [32] M. Gierynska, L. Szulc-Dabrowska, J. Struzik, M.B. Mielcarska, K.P. Gregorzuk-Zboroch, Integrity of the intestinal barrier: the involvement of epithelial cells and microbiota-A mutual relationship, *Animals* 12 (2) (2022), <https://doi.org/10.3390/ani12020145>.
- [33] L. Magnani, M. Colantuoni, A. Mortellaro, Gasdermins: new therapeutic targets in host defense, inflammatory diseases, and cancer, *Front. Immunol.* 13 (2022) 898298, <https://doi.org/10.3389/fimmu.2022.898298>.
- [34] D. Wu, X. Zhu, J. Ao, E. Song, Y. Song, Delivery of ultrasmall nanoparticles to the cytosolic compartment of pyroptotic J774A.1 macrophages via GSDMD(nterm) membrane pores, *ACS Appl. Mater. Interfaces* 13 (43) (2021) 50823–50835, <https://doi.org/10.1021/acsami.1c17382>.
- [35] I.M. Gora, A. Ciechanowska, P. Ladyzynski, NLRP3 inflammasome at the interface of inflammation, endothelial dysfunction, and type 2 diabetes, *Cells-Basel* 10 (2) (2021), <https://doi.org/10.3390/cells10020314>.
- [36] L. Liu, Y. Yang, R. Fang, W. Zhu, J. Wu, X. Li, J.V. Patankar, W. Li, Giardia duodenalis and its secreted PPIB trigger inflammasome activation and pyroptosis in macrophages through TLR4-induced ROS signaling and A20-mediated NLRP3 deubiquitination, *Cells-Basel* 10 (12) (2021), <https://doi.org/10.3390/cells10123425>.
- [37] K.V. Swanson, M. Deng, J.P. Ting, The NLRP3 inflammasome: molecular activation and regulation to therapeutics, *Nat. Rev. Immunol.* 19 (8) (2019) 477–489, <https://doi.org/10.1038/s41577-019-0165-0>.
- [38] H. Xian, Y. Liu, A. Rundberg Nilsson, R. Gatchalian, T.R. Crother, W. G. Tourtellotte, Y. Zhang, G.R. Aleman-Muench, G. Lewis, W. Chen, S. Kang, M. Luevanos, D. Trudler, S.A. Lipton, P. Sorosh, J. Teijaro, J.C. de la Torre, M. Ardit, M. Karin, E. Sanchez-Lopez, Metformin inhibition of mitochondrial ATP and DNA synthesis abrogates NLRP3 inflammasome activation and pulmonary inflammation, *Immunity* 54 (7) (2021) 1463–1477, <https://doi.org/10.1016/j.immuni.2021.05.004>, e11.
- [39] Y.Y. Song, J.M. Song, M. Wang, J.W. Wang, B. Ma, W.L. Zhang, Porcine gasdermin D is a substrate of caspase-1 and an executor of pyroptosis, *Front. Immunol.* 13 (2022), <https://doi.org/10.3389/fimmu.2022.828911>, ARTN 828911.
- [40] H. Loss, J.R. Aschenbach, F. Ebner, K. Tedin, U. Lodemann, Effects of a pathogenic ETEC strain and a probiotic *Enterococcus faecium* strain on the inflammasome response in porcine dendritic cells, *Vet. Immunol. Immunopathol.* 203 (2018) 78–87, <https://doi.org/10.1016/j.vetimm.2018.08.004>.
- [41] A. Di, S. Xiong, Z. Ye, R.K.S. Malireddi, S. Kometani, M. Zhong, M. Mittal, Z. Hong, T.D. Kanneganti, J. Rehman, A.B. Malik, The TWIK2 potassium efflux channel in macrophages mediates NLRP3 inflammasome-induced inflammation, *Immunity* 49 (1) (2018) 56–65 e4, <https://doi.org/10.1016/j.immuni.2018.04.032>.
- [42] S. Zhang, Y. Huang, M. Chen, G. Yang, J. Zhang, Q. Wu, J. Wang, Y. Ding, Q. Ye, T. Lei, Y. Su, R. Pang, R. Yang, Y. Zhang, Characterization of *Escherichia coli* O157: non-H7 isolated from retail food in China and first report of mcr-1/IncI2-carrying colistin-resistant *E. coli* O157:H26 and *E. coli* O157:H4, *Int. J. Food Microbiol.* 378 (2022) 109805, <https://doi.org/10.1016/j.jfoodmicro.2022.109805>.
- [43] Y. Xue, M. Du, M.J. Zhu, Quercetin suppresses NLRP3 inflammasome activation in epithelial cells triggered by *Escherichia coli* O157:H7, *Free Radic. Biol. Med.* 108 (2017) 760–769, <https://doi.org/10.1016/j.freeradbiomed.2017.05.003>.
- [44] Y.S. Xue, M. Du, M.J. Zhu, Raspberry extract prevents NLRP3 inflammasome activation in gut epithelial cells induced by pathogenic *Escherichia coli*, *J. Funct. Foods* 56 (2019) 224–231, <https://doi.org/10.1016/j.jff.2019.03.005>.
- [45] C.E. Diamond, K.W.K. Leong, M. Vacca, J. Rivers-Auty, D. Brough, A. Mortellaro, *Salmonella typhimurium*-induced IL-1 release from primary human monocytes requires NLRP3 and can occur in the absence of pyroptosis, *Sci. Rep.* 7 (1) (2017) 6861, <https://doi.org/10.1038/s41598-017-07081-3>.
- [46] A. Hausmann, D. Bock, P. Geiser, D.L. Berthold, S.A. Fattiger, M. Furter, J. A. Bouman, M. Barthel-Scherrer, C.M. Lang, E. Bakkeren, I. Kolinko, M. Diard, D. Bumann, E. Slack, R.R. Regoes, M. Pilhofer, M.E. Sellin, W.D. Hardt, Intestinal epithelial NAIP/NLRC4 restricts systemic dissemination of the adapted pathogen *Salmonella typhimurium* due to site-specific bacterial PAMP expression, *Mucosal Immunol.* 13 (3) (2020) 530–544, <https://doi.org/10.1038/s41385-019-0247-0>.
- [47] N. Naseer, J. Zhang, R. Bauer, D.A. Constant, T.J. Nice, I.E. Brodsky, I. Rauch, S. Shin, *Salmonella enterica* serovar typhimurium induces NAIP/NLRC4- and NLRP3/ASC-independent, caspase-4-dependent inflammasome activation in human intestinal epithelial cells, *Infect. Immun.* 90 (7) (2022) e0066321, <https://doi.org/10.1128/iai.00663-21>.
- [48] B.I. Arizoz, B. Tastan, E. Tarakcioglu, K.U. Tufekci, M. Olcum, N. Ersoy, A. Bagriyanik, K. Genc, S. Genc, Melatonin attenuates LPS-induced acute depressive-like behaviors and microglial NLRP3 inflammasome activation through the SIRT1/nrf 2 pathway, *Front. Immunol.* 10 (2019) 1511, <https://doi.org/10.3389/fimmu.2019.01511>.
- [49] Z. Liu, X. Wang, S. Ou, M.A. Arowolo, D.X. Hou, J. He, Effects of *Achyranthes bidentata* polysaccharides on intestinal morphology, immune response, and gut microbiome in yellow broiler chickens challenged with *Escherichia coli* K88, *Polymers* 10 (11) (2018), <https://doi.org/10.3390/polym10112333>.
- [50] Q. Yi, J. Liu, Y. Zhang, H. Qiao, F. Chen, S. Zhang, W. Guan, Anethole attenuates enterotoxigenic *Escherichia coli*-induced intestinal barrier disruption and intestinal inflammation via modification of TLR signaling and intestinal microbiota, *Front. Microbiol.* 12 (2021) 647242, <https://doi.org/10.3389/fmicb.2021.647242>.
- [51] X. Song, H. Jiang, Z. Qi, X. Shen, M. Xue, J. Hu, H. Liu, X. Zhou, J. Tu, K. Qi, APEC infection affects cytokine-cytokine receptor interaction and cell cycle pathways in chicken trachea, *Res. Vet. Sci.* 130 (2020) 144–152, <https://doi.org/10.1016/j.rvsc.2020.03.016>.
- [52] C. Huang, Y. Wang, X. He, N. Jiao, X. Zhang, K. Qiu, X. Piao, J. Yin, The involvement of NF- κ B/P38 pathways in *Scutellaria baicalensis* extracts attenuating of *Escherichia coli* K88-induced acute intestinal injury in weaned piglets, *Br. J. Nutr.* 122 (2) (2019) 152–161, <https://doi.org/10.1017/S0007114519000928>.
- [53] C.K. Harvest, E.A. Miao, Autophagy may allow a cell to forgo pyroptosis when confronted with cytosol-invasive bacteria, *Front. Immunol.* 13 (2022), <https://doi.org/10.3389/fimmu.2022.871190>, ARTN 871190.
- [54] V.A.K. Rathinam, Y. Zhao, F. Shao, Innate immunity to intracellular LPS, *Nat. Immunol.* 20 (5) (2019) 527–533, <https://doi.org/10.1038/s41590-019-0368-3>.
- [55] P. Deo, S.H. Chow, M.L. Han, M. Speir, C. Huang, R.B. Schittenhelm, S. Dhital, J. Emery, J. Li, B.T. Kile, J.E. Vince, K.E. Lawlor, T. Naderer, Mitochondrial dysfunction caused by outer membrane vesicles from Gram-negative bacteria activates intrinsic apoptosis and inflammation, *Nat. Microbiol.* 5 (11) (2020) 1418–1427, <https://doi.org/10.1038/s41564-020-0773-2>.
- [56] L.L. Zuo, L.T. Zhou, C.Y. Wu, Y.L. Wang, Y.Y. Li, R. Huang, S.Y. Wu, *Salmonella* spvC gene inhibits pyroptosis and intestinal inflammation to aggravate systemic infection in mice, *Front. Microbiol.* 11 (2020).
- [57] J.C. Santos, D. Boucher, L.K. Schneider, B. Demarco, M. Dilucca, K. Shkarina, R. Heilig, K.W. Chen, R.Y.H. Lim, P. Broz, Human GBP1 binds LPS to initiate assembly of a caspase-4 activating platform on cytosolic bacteria, *Nat. Commun.* 11 (1) (2020) 3276, <https://doi.org/10.1038/s41467-020-16889-z>.
- [58] Z.S. Zajacova, L. Konstantinova, P. Alexa, Detection of virulence factors of *Escherichia coli* focused on prevalence of EAST1 toxin in stool of diarrheic and non-diarrheic piglets and presence of adhesion involving virulence factors in astA positive strains, *Vet. Microbiol.* 154 (3–4) (2012) 369–375, <https://doi.org/10.1016/j.vetmic.2011.07.029>.
- [59] A. Finamore, M. Roselli, A. Imbinto, J. Seeboth, I.P. Oswald, E. Mengheri, *Lactobacillus amylovorus* inhibits the TLR4 inflammatory signaling triggered by enterotoxigenic *Escherichia coli* via modulation of the negative regulators and involvement of TLR2 in intestinal Caco-2 cells and pig explants, *PLoS One* 9 (4) (2014) e94891, <https://doi.org/10.1371/journal.pone.0094891>.